Published in final edited form as:
Magn Reson Med. 2013 July ; 70(1): 97–105. doi:10.1002/mrm.24437.

A Spatially-selective Implementation of the Adiabatic T_2Prep Sequence for Magnetic Resonance Angiography of the Coronary Arteries

Sahar Soleimanifard, MSE[1], **Michael Schär, PhD**[2,3], **Allison G. Hays, MD**[2,4], **Jerry L. Prince, PhD**[1,2], **Robert G. Weiss, MD**[2,4], and **Matthias Stuber, PhD**[1,2,5]

[1]Department of Electrical and Computer Engineering, Johns Hopkins University, Baltimore, MD, USA [2]Russell H. Morgan Department of Radiology and Radiological Science, Division of Magnetic Resonance Research, Johns Hopkins University, Baltimore, MD, USA [3]Philips Healthcare, Cleveland, OH, USA [4]Department of Medicine, Division of Cardiology, Johns Hopkins University, Baltimore, MD, USA [5]Department of Radiology, Centre Hospitalier Universitaire Vaudois, Center for Biomedical Imaging and University of Lausanne, Lausanne, Switzerland

Abstract

In coronary magnetic resonance angiography, a magnetization-preparation scheme for T_2-weighting (T_2Prep) is widely used to enhance contrast between the coronary blood-pool and the myocardium. This pre-pulse is commonly applied without spatial selection to minimize flow sensitivity, but the non-selective implementation results in a reduced magnetization of the in-flowing blood and a related penalty in signal-to-noise-ratio (SNR). It is hypothesized that a spatially-selective T_2Prep would leave the magnetization of blood outside the T_2Prep volume unaffected, and thereby lower the SNR penalty. To test this hypothesis, a spatially-selective T_2Prep was implemented where the user could freely adjust angulation and position of the T_2Prep slab to avoid covering the ventricular blood-pool and saturating the in-flowing spins. A time gap of 150ms was further added between the T_2Prep and other pre-pulses to allow for in-flow of a larger volume of unsaturated spins. Consistent with numerical simulation, the spatially-selective T_2Prep increased *in vivo* human coronary artery SNR (42.3±2.9 vs. 31.4±2.2, n=22, p<0.0001) and contrast-to-noise-ratio (18.6±1.5 vs. 13.9±1.2, p=0.009) as compared to those of the non-selective T_2Prep. Additionally, a segmental analysis demonstrated that the spatially-selective T_2Prep was most beneficial in proximal and mid segments where the in-flowing blood volume was largest compared to the distal segments.

Keywords

Coronary MR Angiography; Contrast Enhancement; T_2Prep; Vessel Conspicuity; In-flowing Blood

Introduction

Non-contrast enhanced three-dimensional (3D) magnetic resonance angiography (MRA) techniques (1) have been widely used to image the geometrically complex coronary arterial anatomy with high spatial resolution and signal-to-noise ratio (SNR). In these techniques,

Corresponding Author: Matthias Stuber, PhD, Rue de Bugnon 46, BH 8.80 10 11, Lausanne, Switzerland, Tel: +41 21 314 7534, Fax: + 41 21 314 46 45, matthias.stuber@chuv.ch.

contrast between the coronary blood-pool and the surrounding tissue is often enhanced by using magnetization preparation schemes (2–5). For contrast enhancement between the coronary blood-pool and the myocardium, a magnetization-preparation scheme for T_2-weighting (T_2Prep) that takes advantage of T_2 differences between arterial blood and myocardial tissue has been proposed (3). This pre-pulse was originally designed in a spatially non-selective fashion to minimize flow sensitivity. Recently, a B_0- and B_1-insensitive variant of it, using adiabatic refocusing pulses, has been proposed for high-field systems (6). However, independent of the field strength, this spatially non-selective implementation affects the steady-state magnetization of the spins both inside and outside the imaged volume. Therefore, the magnetization of the blood flowing into the imaged slice is reduced and inevitably leads to a penalty in coronary SNR (7). A significant fraction of the blood-volume that enters the coronary arteries in diastole after aortic valve closure originates from the ascending aorta. We hypothesize that a properly placed spatially-selective variant of the T_2Prep that does not affect the blood-pool magnetization above the aortic valve would allow blood with fully recovered magnetization to flow into the coronary arteries and improve SNR. The purpose of this work was to test this hypothesis and investigate if the physiology can be exploited to improve vessel conspicuity. Thereby, a carefully designed and graphically-prescribed spatially-selective variant of this pre-pulse was implemented and its performance studied quantitatively.

In the pursuit of this goal, we performed numerical simulations of the Bloch equations to compare the potential signal gain from in-flowing blood between spatially-selective and non-selective variants of the T_2Prep. Subsequently, we developed and implemented a flow-compensated spatially-selective T_2Prep. Finally, we acquired *in vivo* human coronary MRA with both the spatially-selective T_2Prep and its conventional non- selective counterpart and we compared the results quantitatively.

Methods

Background

The conventional T_2Prep (3) is designed to "store" T_2-weighted magnetization in the longitudinal direction prior to imaging. This T_2-weighted magnetization increases contrast between the coronary blood-pool and its surroundings since the T_2 of arterial blood is much longer than those of venous blood and myocardium. Fig. 1a shows the schematic of the non-selective T_2Prep. The T_2-weighting is created by first exciting the magnetization with a non-selective 90° RF pulse after which the magnetization is exposed to T_2-decay in the transverse plane, and next storing the resultant magnetization in the longitudinal direction using a non-selective 90° tip-up RF pulse after a time interval (TE). During TE, the transverse magnetization is repeatedly refocused by adiabatic 180° RF pulses to minimize the effects of B_0 and B_1 inhomogeneities (6). A relatively large spoiling gradient follows to dephase residual transverse magnetization. Fig. 1b illustrates the integration of the T_2Prep as part of a contemporary fat suppressed free-breathing navigator-gated and corrected 3D coronary MRA imaging approach (8).

Numerical Simulation

To study the potential signal gain obtained from in-flowing blood into the coronary arteries using a spatially- selective variant of the T_2Prep under ideal and well-controlled conditions, a numerical simulation of the Bloch equations (9) was implemented using MATLAB (MathWorks, Natick, MA, USA) as shown in Fig. 2. With this tool, the longitudinal magnetization $M_z(t)$ of both myocardium and blood were calculated as a function of time for the pulse sequence shown in Fig. 1b. While the effect of other pre-pulses (navigator, fat suppression, saturation slab) on $M_z(t)$ was neglected in our calculations, the total duration of

these pulses was still taken into account. The simulation modeled a cardiac-gated gradient echo sequence with a heart rate of 60bpm in a 3.0T MR scanner. Simulation parameters were as follows: T_{1blood} = 1550ms, T_{2blood} = 140ms, $T_{1myocardium}$ = 1115ms, $T_{2myocardium}$ = 55ms (6,10,11), RF excitation angle = 20°, 25 RF excitations per k-space segment, TE of T_2Prep = 50ms, duration of other pre-pulses (T_{prep}) = 50ms. The effect of all RF excitations in the acquisition window was taken into account for this simulation. However, we only considered the first readout, corresponding to the signal in the center of k-space, for comparison of in-flowing blood magnetization between the two variants of T_2Prep.

Spatially-selective Adiabatic T_2Prep

We implemented the spatially-selective T_2Prep by replacing the two non-selective 90° RF pulses with spatially-selective versions as shown in Fig. 1c. In addition, flow-compensating gradients using gradient moment nulling were added to minimize flow sensitivity of the pre-pulse. Further, a time gap (T_{gap}) was added between the T_2Prep sequence and other pre-pulses (Fig. 1d). This delay can be increased by the user to allow for in-flow of a larger volume of spins with fully relaxed magnetization into the coronary arteries.

In the numerical simulations, it is assumed that in-flowing blood-pool magnetization is not affected by the spatially-selective T_2Prep prior to entering into the imaged volume. However, this assumption may not be entirely valid if the spatially-selective T_2Prep has the same orientation and position as the imaged volume, which in many cases is selected in a way that it covers the ascending aorta. To address this issue and to avoid T_2-preparation of the aortic blood-pool before it flows into the coronary arteries, the orientation, position, and slice thickness of the spatially-selective T_2Prep volume can be freely selected by the user on the scanner console. Fig. 3c illustrates the T_2Prep volume selected along the axis of the artery of interest and orthogonal to the imaged volume without covering the ventricular blood-pool or the ascending aorta.

In vivo Imaging Protocol and Hardware

A total of 14 healthy adult subjects with no history of cardiovascular disease (mean age 32±11 years; 11 men) were recruited for the study. The protocol was approved by the Johns Hopkins Institutional Review Board and written informed consent was obtained from all participants. Studies were performed on a commercial whole body 3.0T MR scanner (Achieve R3.2, Philips Healthcare, Best, The Netherlands) equipped with a thirty-two-channel cardiac phased-array coil, multi-transmit system, and vector electrocardiography triggering (12). The duration of the entire study was approximately 45 minutes.

All subjects were scanned in the supine position with vector electrocardiography electrodes connected to the anterior thorax. The imaging protocol began with a multi-slice segmented k-space gradient echo scout scan in axial, sagittal, and coronal views to identify the heart and the lung-liver interface for navigator localization. This scan was followed by a sensitivity encoding (13) reference scan. Subsequently, an axial mid-ventricular balanced steady-state free-precession cine scan (14) was obtained during free- breathing to visually identify the period of minimal coronary motion. The beginning of this stationary period was chosen as trigger delay for subsequent scans in the protocol. The cine scan was followed by the coronary localizer scan, a quick low spatial resolution navigator-gated and corrected whole-heart 3D scout scan, oriented axially during free-breathing, which was utilized for planning of the subsequent high spatial resolution 3D coronary artery acquisitions using the three-point plan scan tool (8). Using two-dimensional sensitivity encoding, the duration of the localizer scan was below 2 minutes (navigator efficiency ~40%). As a result, localization of coronaries and T_2Prep slab planning led to approximately 5 minutes of scan preparation in total. When the image quality on the scout scan was equivalent for the right coronary

artery (RCA) and the left anterior descending artery (LAD), both arteries were subsequently imaged and analyzed.

3D Coronary Artery Imaging Sequence

After localizing the coronary arteries, 3D volume-targeted navigator-gated (gating window = 5mm) and corrected (correction factor of 0.6 in the superior-inferior direction (15)) MRA of the coronary arteries (8) was obtained during free-breathing. A conventional 3D segmented k-space spoiled gradient echo with fractional echo readout and centric k-space profile ordering was used. Imaging parameters were as follows: repetition time = 4.1ms, echo time = 1.5ms, field-of-view = 300×300×20mm^3, acquired voxel size = 0.86×0.86×4.00mm^3, reconstructed voxel size = 0.78×0.78×2.00mm^3, RF excitation angle = 20°, 25 RF excitations per k-space segment (with an acquisition window of 103ms), and a sensitivity encoding acceleration factor of 2. A spectrally selective fat saturation pre-pulse was applied both before the navigator and before the imaging sequence. In addition, an anterior saturation slab preceded the imaging sequence to suppress respiratory motion artifacts originating from the chest wall. The combined duration of these pre-pulses was 50ms as shown in Fig. 1b. Two adiabatic refocusing pulses and a TE of 50ms were chosen for both variants of T_2Prep implementations (6). The 3D coronary MRA were acquired a) without T_2Prep, b) with non-selective T_2Prep, and c) with the proposed spatially-selective T_2Prep in all subjects. In a few initial volunteers, the T_{gap} between the T_2Prep and other pre-pulses that leads to best visual vessel conspicuity was experimentally determined by increasing the T_{gap} from 0ms to 200ms in increments of 50ms. A T_{gap} of 150ms was found to allow for a large volume of in-flowing blood with no significant decrease in T_2 contrast and thus was used for the spatially-selective sequence. Moreover, additional images using the spatially-selective T_2Prep with zero time gap were acquired in 7 volunteers to test the effect of T_{gap} on the resultant SNR. Since quantification of SNR is not straightforward on sensitivity encoding accelerated images (16), additional 3D fast noise scans (~9sec) with disabled RF excitations and gradients but otherwise identical scan settings were acquired immediately following all the 3D coronary MRA acquisitions for SNR measurements as previously described (17).

Image Analysis

On each coronary artery of interest, vessel boundaries were identified using a semi-automated algorithm developed in-house (18). The vessel neighborhood region was defined as the outer two voxels of vessel boundaries (i.e. a rim with thickness of about 2.3mm). To identify this region, the segmented vessel boundaries were first dilated using a five-voxel morphological dilation operator. Subtraction of the inner vessel region from the dilated mask then yielded the neighborhood regions.

Three coronary artery segments were defined in a modified form according to the recommendations of the American Heart Association (19). The segments were categorized into three groups: proximal, mid, and distal as illustrated in Fig. 4 that shows examples for both the RCA and LAD.

For each segment, the signal was averaged on the anatomical images both inside the vessel boundaries ($S_{image,vessel}$), and the neighborhood region ($S_{image,neighborhood}$). Subsequently, vessel boundary and neighborhood contours were copied onto the corresponding noise scans where noise measurements were obtained. Vessel SNR was then defined as

$$SNR = \frac{S_{\text{image,vessel}}}{S_{\text{noise,vessel}}} \quad (1)$$

where $SD_{noise,vessel}$ is the standard deviation of the noise measurements inside the vessel boundaries.

The vessel region and its adjacent neighborhood were selected to define vessel-neighborhood CNR as

$$CNR=\frac{S_{\text{image,vessel}}-S_{\text{image,neighborhood}}}{SD_{\text{noise,vessel+neighborhood}}} \quad (2)$$

where $SD_{noise,vessel+neighborhood}$ is the standard deviation of noise measurements inside the vessel boundaries and its immediate neighborhood.

Vessel sharpness was measured in each coronary segment using the first-order derivative of the multi-planar reformatted MRA images, as previously described (20).

Statistical Analysis

Statistical analysis was performed using JMP software (version 8, SAS Institute Inc., Carey, NC). All segments were included in the analysis and results are reported as mean ± one standard error of mean. Analysis of variance (ANOVA) with Tukey post hoc test was used to analyze repeated measures of vessel SNR, vessel-neighborhood CNR, and vessel sharpness in acquisitions with no T_2Prep, non-selective T_2Prep, and the proposed spatially-selective T_2Prep with T_{gap}=150ms. Paired two-tailed Student's t-test was used to compare vessel SNR in the spatially-selective T_2Prep images acquired with T_{gap}=0 and T_{gap}=150ms. A p-value of <0.05 was considered statistically significant in all analyses.

Results

Numerical Simulation

The longitudinal magnetization $M_z(t)$ of blood and myocardium for the 3D coronary MRA sequence (as shown in Fig. 1b) is illustrated in Fig. 2a. The solid black line shows the magnetization of myocardium for multiple consecutive cardiac cycles. The blue and red lines refer to the longitudinal magnetization of blood outside the imaged volume, which flows into the coronary arteries in the non- selective and spatially-selective variants of T_2Prep, respectively. The black rectangle in Fig. 2a is zoomed and shown in Fig. 2b to better compare the magnetization from in-flowing blood between the two implementations. The horizontal lines refer to the magnetization that is available for the first RF excitation used for imaging. This magnetization corresponds to the signal in the center of k- space.

In-flowing Blood: Non-selective T_2Prep

The horizontal blue line shows magnetization at the first readout for the in-flowing blood that enters the imaged volume before the beginning of the T_2Prep pre-pulse (Ta). This in-flowing blood always experiences the non- selective T_2Prep outside the imaged volume in previous RR intervals and its magnetization is $0.50M_0$ when entering the imaged volume. The in-flowing blood entering the imaged volume between Ta and the beginning of the imaging sequence (Tb) has the same magnetization since the blood is always affected by the pre-pulse regardless whether it is inside or outside the imaged volume.

In-flowing Blood: Spatially-selective T_2Prep without T_{gap}

By comparison, the in-flowing blood entering the imaged volume before Ta for the spatially-selective variant of the T_2Prep experiences only one T_2Prep and enters the imaged volume with a magnetization of $0.67M_0$ (Fig. 2b, horizontal dashed red line), and results in 34% increase of blood magnetization when compared to the non-selective T_2Prep (Fig. 2b,

M_z=0.50M_0, horizontal blue line). The in-flowing blood, which enters the imaged volume between Ta and Tb is not affected by the T_2Prep (Fig. 2b, horizontal solid red line), and thus possesses maximum magnetization. However, blood must flow into the artery between the end of the T_2Prep and the beginning of the imaging sequence (T_{prep}= 50ms; see Fig. 1b) to achieve this maximum magnetization gain. In addition, the in-flowing blood is not expected to entirely replace the blood in the arteries at every heartbeat (21) and the difference in the in-flowing blood magnetization of the two T_2Prep implementations decreases after the first cardiac cycle (Fig. 2b, red and blue lines in the dashed black circle). For these reasons, the resultant SNR gain in the final image is expected to be smaller than the in-flowing blood magnetization gain of 34%.

In-flowing Blood: Spatially-selective T_2Prep with T_{gap}

Fig. 2c and 2d show the same situation as in Fig. 2a and 2b but with an added T_{gap} of 150ms. Due to T_1 relaxation, the additional T_{gap} in the spatially-selective scenario results in 40% increase of blood magnetization from spins observing one T_2Prep and entering the imaged volume before Ta as compared with in-flowing blood for the non- selective pre-pulse (M_z=0.70M_0, horizontal dashed red line in Fig. 2d, vs. M_z=0.50M_0, horizontal solid blue line in Fig. 2b). The addition of T_{gap} between the T_2Prep and other pre-pulses may allow for a larger volume of spins to flow into the imaged volume between Ta and Tb without T_2 preparation (horizontal solid red line in Fig. 2d). The fully relaxed spins may potentially compensate for loss of magnetization from blood remaining in the coronary arteries for more than one heartbeat, and lead to a larger signal gain. If this gap is chosen too large, however, prolonged T_1 relaxation of the myocardium may lead to a reduced blood-muscle contrast.

In vivo Experiments

A total of 22 coronary arteries (RCA: n=13; LAD: n=9) were imaged in 14 healthy adult subjects using the spatially-selective sequence with nonzero T_{gap}. The duration for each 3D MRA scan was approximately 2 minutes (navigator efficiency ~40%). The proximal and mid coronary segments were visible in every dataset and the distal segments were identified in 8 datasets. In addition, 7 coronary arteries (RCA: n=5; LAD: n=2) were imaged using the spatially-selective sequence with T_{gap}=0. Fig. 3 shows examples of multi- planar reformatted (20) images of RCA and LAD in three subjects, acquired without a T_2Prep, with non-selective T_2Prep, and with the proposed spatially-selective T_2Prep (T_{gap} = 150ms). The quantitative endpoints of this study averaged for proximal, mid, and distal coronary segments are summarized in Table 1.

Signal-to-Noise-Ratio

Both selective and non-selective implementations led to a vessel SNR penalty as compared to imaging without T_2Prep ($p<0.001$), as previously reported (3,7). In the subset of images acquired with T_{gap}=0, mean SNR improved by 22% in comparison with paired images acquired with the conventional non-selective sequence (37.6±4.6 vs. 30.9±3.8, p=0.018, n=7). With the addition of $T_{gap,}$ a larger in-flow volume of unsaturated spins further increased SNR as shown in Table 1, consistent with numerical simulations. The spatially-selective T_2Prep with T_{gap}=150ms led to 35% higher vessel SNR when compared to non-selective T_2Prep (42.3±2.9 vs. 31.4±2.2, $p<0.0001$, n=22). Segmental analysis of SNR (as shown in Fig. 5a) revealed that in spatially-selective T_2prep (with T_{gap}=150ms) images, a 40% increase in SNR was achieved in proximal segments (47.0±5.0 vs. 33.6±3.7, p=0.0006). This result shows that T_{gap} allowed in-flow of sufficient volume of unsaturated spins to attenuate the loss from remaining spins in these coronary segments from previous heartbeats, in agreement with numerical simulations. Additionally, a smaller SNR increase of 32% was achieved in mid segments (spatially-selective with T_{gap}=150ms: 37.9±4.3 vs.

non-selective: 28.6±3.4, p=0.008). A similar trend with 26% increase in SNR was also observed in the distal segments (spatially-selective with T_{gap}=150ms: 40.4±5.0 vs. non-selective: 32.0±4.4, p=NS).

Contrast-to-Noise-Ratio

Similar to SNR findings, vessel-neighborhood CNR measurements increased by 33% using the spatially- selective T_2Prep in comparison with its non-selective counterpart (18.6±1.5 vs. 13.9±1.2, p=0.0087), although smaller compared to imaging without T_2Prep (p<0.001). Segmental CNR decreased as well in proximal and mid segments with use of both T_2Prep pre-pulses (p<0.001) as shown in Fig. 5b. However, the proposed spatially-selective T_2Prep increased CNR significantly in these segments as compared to the non-selective T_2Prep (proximal: 19.8±2.4 vs. 14.1±2.0, p=0.0025; mid: 18.2±2.5 vs. 13.1±2.0, p=0.028). The CNR of distal segments was similar for both implementations of T_2Prep (spatially-selective: 16.2±2.2; non-selective: 15.4±2.1 p=NS).

Vessel Sharpness

Both variants of T_2Prep increased the overall sharpness of coronary arteries in comparison to imaging without T_2Prep (p<0.0001, Table 1). Images acquired with the spatially-selective T_2Prep exhibited somewhat higher overall vessel sharpness compared to the conventional implementation (49.8±0.9% vs. 46.2±1.2%, p=0.061). This increase was found to be significant in proximal segments (49.6±1.2% vs. 44.7±1.6%, p=0.0097).

Discussion

The T_2Prep pre-pulse, widely used in coronary MRA (7,8,22–24), has been optimized for insensitivity to flow artifacts (3) and field inhomogeneities (6). However, its conventional non-selective implementation inevitably leads to a penalty in SNR (7). We hypothesized that a spatially-selective variant of this pre- pulse, leaving the magnetization of blood in great vessels and heart chambers unaffected, leads to a higher signal in the coronary blood-pool, which may in part compensate for the loss in SNR. Therefore, we proposed, implemented, and tested a spatially-selective T_2Prep at 3.0T.

In this modified T_2Prep an additional T_{gap}=150ms was added between T_2Prep and other pre-pulses (Fig. 1d) to allow for a larger volume of spins with maximum magnetization to flow into the imaged volume. Additionally, the orientation and position of the spatially-selective slab could be freely selected by the user (Fig. 3c). This configuration has a twofold advantage. It not only avoids saturation of the spins in ascending aorta before flowing into the coronary arteries, but it may also minimize the flow artifacts in ventricular blood-pool if the T_2Prep volume is selected in a way that it does not fully cover the ventricles. An acknowledged limitation of this implementation is that the T_2Prep volume must be planned along the main axes of the arteries on the coronary localizer scan. Although the positioning of slabs is a fairly straightforward procedure on most commercial scanners, this adds 2–3 minutes to the scan. The time required for the coronary localization and slab positioning together results in approximately 5 minutes of scan preparation, which could be used for other signal enhancing strategies such as signal averaging or acquisition of a larger volume with conventional T_2Prep. Whether those strategies result in similarly improved vessel conspicuity or CNR remains to be studied, however.

Improvements in SNR, CNR, and vessel sharpness using the proposed spatially-selective T_2Prep were observed in healthy coronary arteries. In agreement with numerical simulations of the Bloch equations, the spatially- selective T_2prep with a T_{gap} improved mean SNR, as compared with the conventional non-selective T_2prep, by 35% (p<0.0001) averaged in the

three coronary segments and by 40% (p=0.0006) in proximal segments (Table 1). In mid and distal segments, in which smaller volumes of in-flowing blood were expected, a smaller SNR improvement was observed. In the absence of T_{gap}, the spatially- selective T_2prep improved the overall SNR by 22% compared to the conventional non-selective T_2Prep, somewhat smaller than the 34% magnetization gain computed with numerical simulations. We speculate that this discrepancy is due to the remaining blood in coronaries from previous heartbeats.

T_2Prep has been shown to improve blood-myocardium CNR (7). However, in the present study, and as a result of the T_2Prep volume that was orthogonal to the imaged volume, the coverage of blood-pool and myocardium in the images was small (as shown in the examples in Fig. 3). Therefore, we chose to quantify the CNR between the coronary blood-pool and its immediate surroundings instead (as shown in Fig. 4). This regional assessment of contrast may be more representative of vessel conspicuity compared with the common analysis of contrast using manually drawn regions of interest in aorta and myocardial wall. Results from this study demonstrated that the proposed implementation of T_2Prep improved the regional CNR by 33% (p=0.0087) in comparison with the non-selective implementation.

Additionally, the T_2Prep improved vessel sharpness ($p<0.05$) compared to imaging without T_2Prep. The spatially-selective T_2Prep, taking advantage of in-flowing blood, further increased the vessel sharpness values compared with the non-selective implementation and confirmed that the introduction of T_{gap} and its minor resultant reduction in T_2-weighting did not decrease vessel conspicuity. The major beneficiaries of the new implementation were the proximal and mid segments of the coronary arteries where the in-flowing blood volume was largest compared to the more distal segments. These segments are routinely visualized with MRA, especially the proximal segments that are evaluable in nearly 100% of subjects with an excellent agreement between MRA and conventional angiography (1).

As suggested by the results, the proposed implementation may result in flow-dependent non-uniformly enhanced arterial segments in an artery of interest. Indeed, reduced blood-flow in the region of a lumen-narrowing stenosis may have an impact on the contrast in adjacent vessel segments using the proposed T_2Prep. Systemic evaluation of this technique in CAD patients and whether it affects detection of stenosis is beyond the scope of this work. However, and based on the encouraging results in this initial study, this remains to be investigated in a patient cohort in comparison to non- selective T_2Prep and the gold standard x-ray angiography.

In this work, the new selective implementation of T_2Prep was examined with a volume-targeted imaging sequence to test whether the physiology can be utilized to improve conspicuity of coronary arteries in MRA. Additionally, and if the spatially-selective T_2Prep does not affect the magnetization of the blood-pool above the aortic valve, a benefit may be expected for whole-heart imaging. However, this benefit is likely to be reduced for whole-heart imaging, as the selective implementation is most effective when the T_2Prep volume is small and avoids intersection with the ascending aorta. Alternatively, and owing to the fact that the left coronary system may benefit more from the T_2Prep than the RCA which is often embedded in fat, a targeted T_2Prep could be selectively applied for the left coronary system during whole-heart imaging. Simultaneously, sub-dividing the entire whole-heart volume into smaller sub-volumes may be another option to take advantage of a spatially-selective T_2Prep for whole-heart imaging. The practical use of this approach and its magnitude of enhancement remain to be investigated with the whole-heart approach. Nevertheless, volume-targeted coronary MRA continues to be a valuable alternative to whole-heart imaging at high magnetic field strengths (25).

Limitations

One limitation to this study is that we did not evaluate the addition of T_{gap} in the non-selective sequence. However, as shown in the numerical simulation, the blood flowing into the imaged volume before or after T_2Prep never recovers to its maximum magnetization in the non-selective implementation such that a T_{gap} in this setting would only result in T_1 relaxation and a reduction of the blood-myocardium contrast. Furthermore, distal segments were identified in only eight datasets and lack of significance in results may be in part due to the small sample size. Also the difference in sample size for images acquired with and without T_{gap} prevented a head to head comparison. Lastly, no studies were conducted in patients with coronary artery disease. However, the implementation is complete and the efficacy of the technique can now be readily tested in different populations.

Conclusions

This study tested the hypothesis that a spatially-selective variant of the T_2Prep pulse leads to improved SNR in non-contrast enhanced coronary MRA. Consistent with the results from a numerical simulation, significantly improved SNR and CNR were found in *in vivo* coronary artery images where it was demonstrated that proximal and mid segments of the coronary arterial tree are among the major beneficiaries of this new technique.

Acknowledgments

This work was supported in part by the National Institutes of Health/National Heart, Lung, and Blood Institute research grants RO1HL084186 and ARRA 3R01Hl084186-04S1.

References

1. Chiribiri A, Ishida M, Nagel E, Botnar RM. Coronary Imaging With Cardiovascular Magnetic Resonance: Current State of the Art. Progress in Cardiovascular Diseases. 2011; 54(3):240–252. [PubMed: 22014491]
2. Li D, Paschal CB, Haacke EM, Adler LP. Coronary arteries: three-dimensional MR imaging with fat saturation and magnetization transfer contrast. Radiology. 1993; 187(2):401–406. [PubMed: 8475281]
3. Brittain JH, Hu BS, Wright GA, Meyer CH, Macovski A, Nishimura DG. Coronary Angiography with Magnetization-Prepared T2 Contrast. Magnetic Resonance in Medicine. 1995; 33(5):689–696. [PubMed: 7596274]
4. Edelman RR, Manning WJ, Burstein D, Paulin S. Coronary arteries: breath-hold MR angiography. Radiology. 1991; 181(3):641–643. [PubMed: 1947074]
5. Stuber M, Botnar RM, Spuentrup E, Kissinger KV, Manning WJ. Three-dimensional high-resolution fast spin-echo coronary magnetic resonance angiography. Magnetic Resonance in Medicine. 2001; 45(2):206–211. [PubMed: 11180427]
6. Nezafat R, Stuber M, Ouwerkerk R, Gharib AM, Desai MY, Pettigrew RI. B1-insensitive T2 preparation for improved coronary magnetic resonance angiography at 3 T. Magnetic Resonance in Medicine. 2006; 55(4):858–864. [PubMed: 16538606]
7. Botnar RM, Stuber M, Danias PG, Kissinger KV, Manning WJ. Improved Coronary Artery Definition With T2-Weighted, Free-Breathing, Three-Dimensional Coronary MRA. Circulation. 1999; 99(24):3139–3148. [PubMed: 10377077]
8. Stuber M, Botnar RM, Danias PG, Sodickson DK, Kissinger KV, Van Cauteren M, De Becker J, Manning WJ. Double-oblique free-breathing high resolution three-dimensional coronary magnetic resonance angiography. Journal of the American College of Cardiology. 1999; 34(2):524–531. [PubMed: 10440168]
9. Bloch F. Nuclear Induction. Physical Review. 1946; 70(7–8):460–474.

10. Schär M, Kozerke S, Fischer SE, Boesiger P. Cardiac SSFP imaging at 3 Tesla. Magnetic Resonance in Medicine. 2004; 51(4):799–806. [PubMed: 15065254]
11. Stanisz GJ, Odrobina EE, Pun J, Escaravage M, Graham SJ, Bronskill MJ, Henkelman RM. T1, T2 relaxation and magnetization transfer in tissue at 3T. Magnetic Resonance in Medicine. 2005; 54(3):507–512. [PubMed: 16086319]
12. Fischer SE, Wickline SA, Lorenz CH. Novel real-time R-wave detection algorithm based on the vectorcardiogram for accurate gated magnetic resonance acquisitions. Magnetic Resonance in Medicine. 1999; 42(2):361–370. [PubMed: 10440961]
13. Pruessmann KP, Weiger M, Scheidegger MB, Boesiger P. SENSE: Sensitivity encoding for fast MRI. Magnetic Resonance in Medicine. 1999; 42(5):952–962. [PubMed: 10542355]
14. Oppelt A, Graumann R, Barfuss H, Fischer H, Hartl W, Schajor W. FISP ▫ new fast MRI sequence. Electromedica. 1986; 54:15–18.
15. Wang Y, Riederer SJ, Ehman RL. Respiratory Motion of the Heart: Kinematics and the Implications for the Spatial Resolution in Coronary Imaging. Magnetic Resonance in Medicine. 1995; 33(5):713–719. [PubMed: 7596276]
16. Dietrich O, Raya JG, Reeder SB, Reiser MF, Schoenberg SO. Measurement of signal-to-noise ratios in MR images: Influence of multichannel coils, parallel imaging, and reconstruction filters. Journal of Magnetic Resonance Imaging. 2007; 26(2):375–385. [PubMed: 17622966]
17. Yu J, Agarwal H, Stuber M, Schär M. Practical signal-to-noise ratio quantification for sensitivity encoding: Application to coronary MR angiography. Journal of Magnetic Resonance Imaging. 2011; 33(6):1330–1340. [PubMed: 21591001]
18. Soleimanifard S, Schaär M, Hays AG, Weiss RG, Stuber M, Prince JL. Vessel Centerline Tracking and Boundary Segmentation in Coronary MRA with Minimal Manual Interaction. IEEE International Symposium on Biomedical Imaging: From Nano to Macro. 2012:1417–1420. [PubMed: 23032185]
19. Austen WG, Edwards JE, Frye RL, Gensini GG, Gott VL, Griffith LS, McGoon DC, Murphy ML, Roe BB. A reporting system on patients evaluated for coronary artery disease. Report of the Ad Hoc Committee for Grading of Coronary Artery Disease, Council on Cardiovascular Surgery, American Heart Association. Circulation. 1975; 51(4 Suppl):5–40. [PubMed: 1116248]
20. Etienne A, Botnar RM, van Muiswinkel AMC, Boesiger P, Manning WJ, Stuber M. “Soap-Bubble” visualization and quantitative analysis of 3D coronary magnetic resonance angiograms. Magnetic Resonance in Medicine. 2002; 48(4):658–666. [PubMed: 12353283]
21. Sabbah HN, Khaja F, Brymer JF, Hawkins ET, Stein PD. Blood velocity in the right coronary artery: Relation to the distribution of atherosclerotic lesions. The American Journal of Cardiology. 1984; 53(8):1008–1012. [PubMed: 6702675]
22. Kim WY, Danias PG, Stuber M, Flamm SD, Plein S, Nagel E, Langerak SE, Weber OM, Pedersen EM, Schmidt M, Botnar RM, Manning WJ. Coronary Magnetic Resonance Angiography for the Detection of Coronary Stenoses. New England Journal of Medicine. 2001; 345(26):1863–1869. [PubMed: 11756576]
23. Shea SM, Deshpande VS, Chung Y-C, Li D. Three-dimensional true-FISP imaging of the coronary arteries: Improved contrast with T2-preparation. Journal of Magnetic Resonance Imaging. 2002; 15(5):597–602. [PubMed: 11997902]
24. Liu C-Y, Bley TA, Wieben O, Brittain JH, Reeder SB. Flow-independent T2-prepared inversion recovery black-blood MR imaging. Journal of Magnetic Resonance Imaging. 2010; 31(1):248–254. [PubMed: 20027595]
25. van Elderen SGC, Versluis MJ, Westenberg JJM, Agarwal H, Smith NB, Stuber M, de Roos A, Webb AG. Right Coronary MR Angiography at 7 T: A Direct Quantitative and Qualitative Comparison with 3 T in Young Healthy Volunteers 1. Radiology. 2010; 257(1):254–259. [PubMed: 20851943]

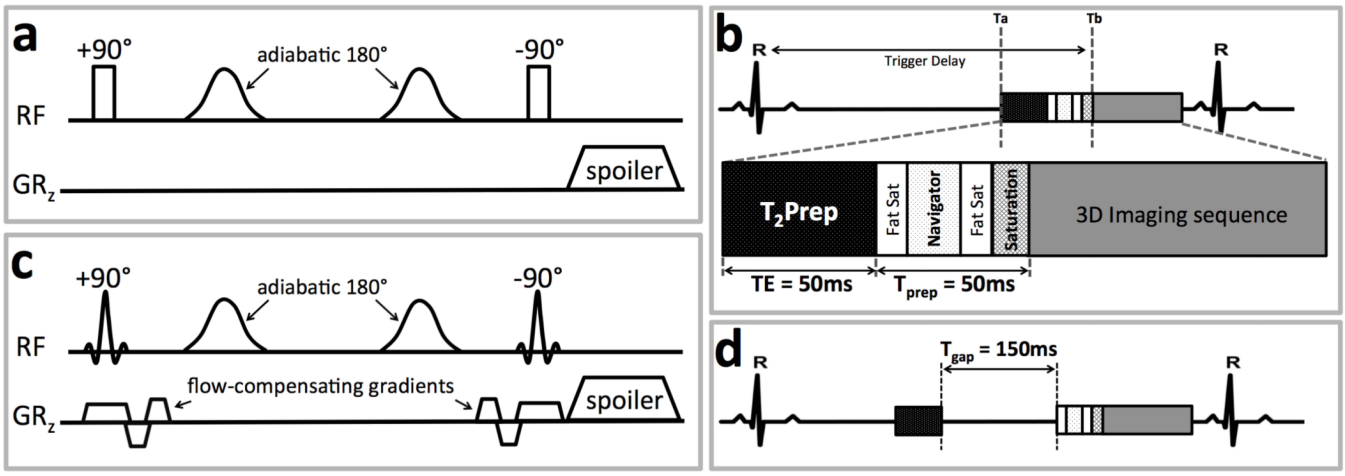

Figure 1.

(a) Non-selective T_2Prep pre-pulse illustrated with two adiabatic refocusing pulses. GR_z: the slice-select gradient. **(b)** Schematic of pulse sequences for the three-dimensional navigator - gated coronary MRA used for *in vivo* experiments. Fat Sat: fat saturation pre-pulse, Saturation: saturation slab pre-pulse. **(c)** The proposed spatially-selective T_2Prep with selective 90° RF pulses and additional flow-compensating gradients. **(d)** A time interval T_{gap} added between T_2Prep and other pre-pulses to allow for a larger volume of blood with fully relaxed magnetization flowing into the imaged volume.

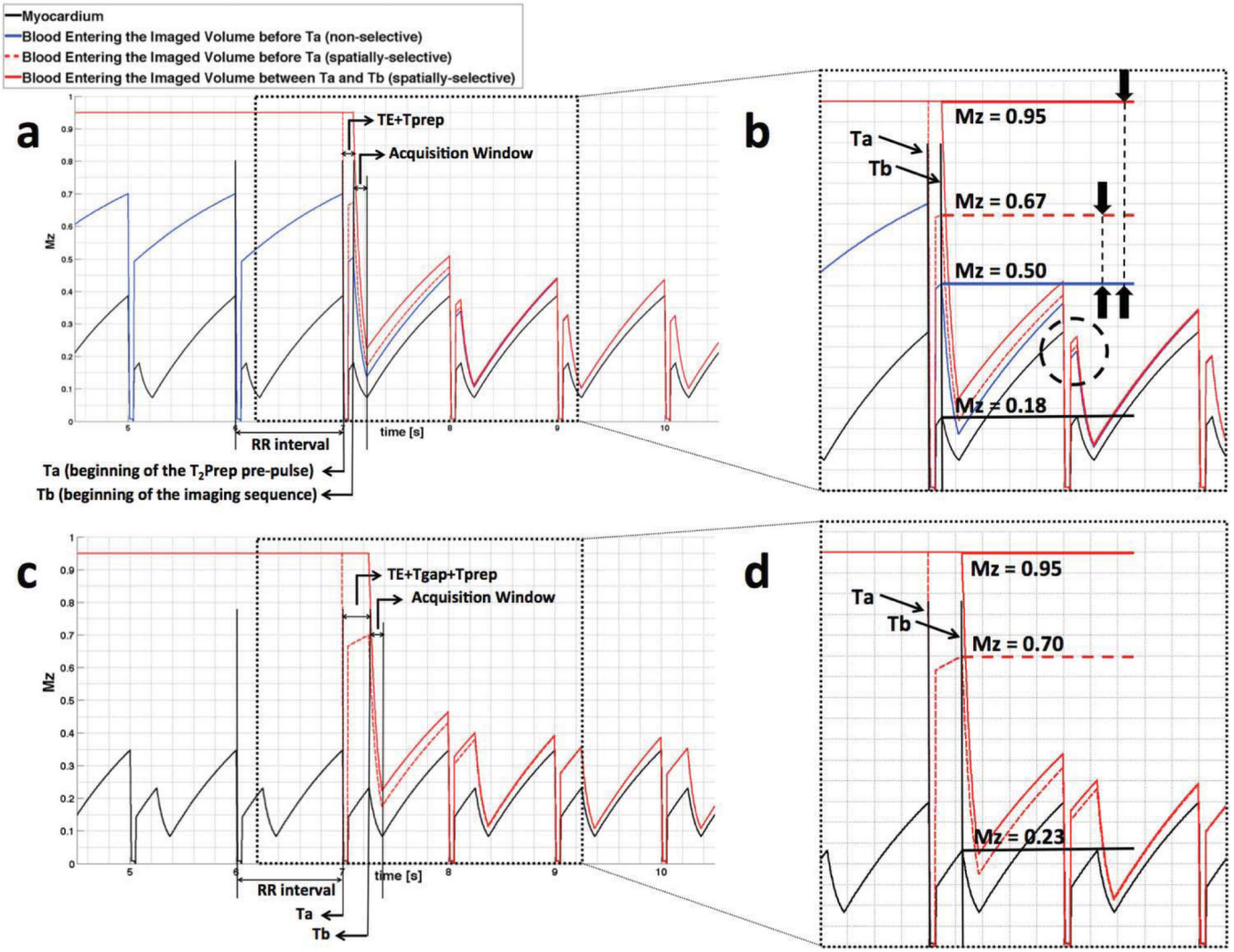

Figure 2.

Longitudinal magnetization in myocardium and in-flowing blood in a 3D cardiac-gated gradient echo imaging sequence as shown in Fig. 1 with **(a)**, **(b)** $T_{gap} = 0$ and **(c)**, **(d)** $T_{gap} = 150$ms. Ta and Tb mark the beginning of the T_2Prep and the imaging sequence, respectively. Dotted rectangles in **(a)** and **(c)** are magnified and shown in **(b)** and **(d)** to demonstrate the magnetization of in-flowing blood when entering the imaged volume (horizontal lines).

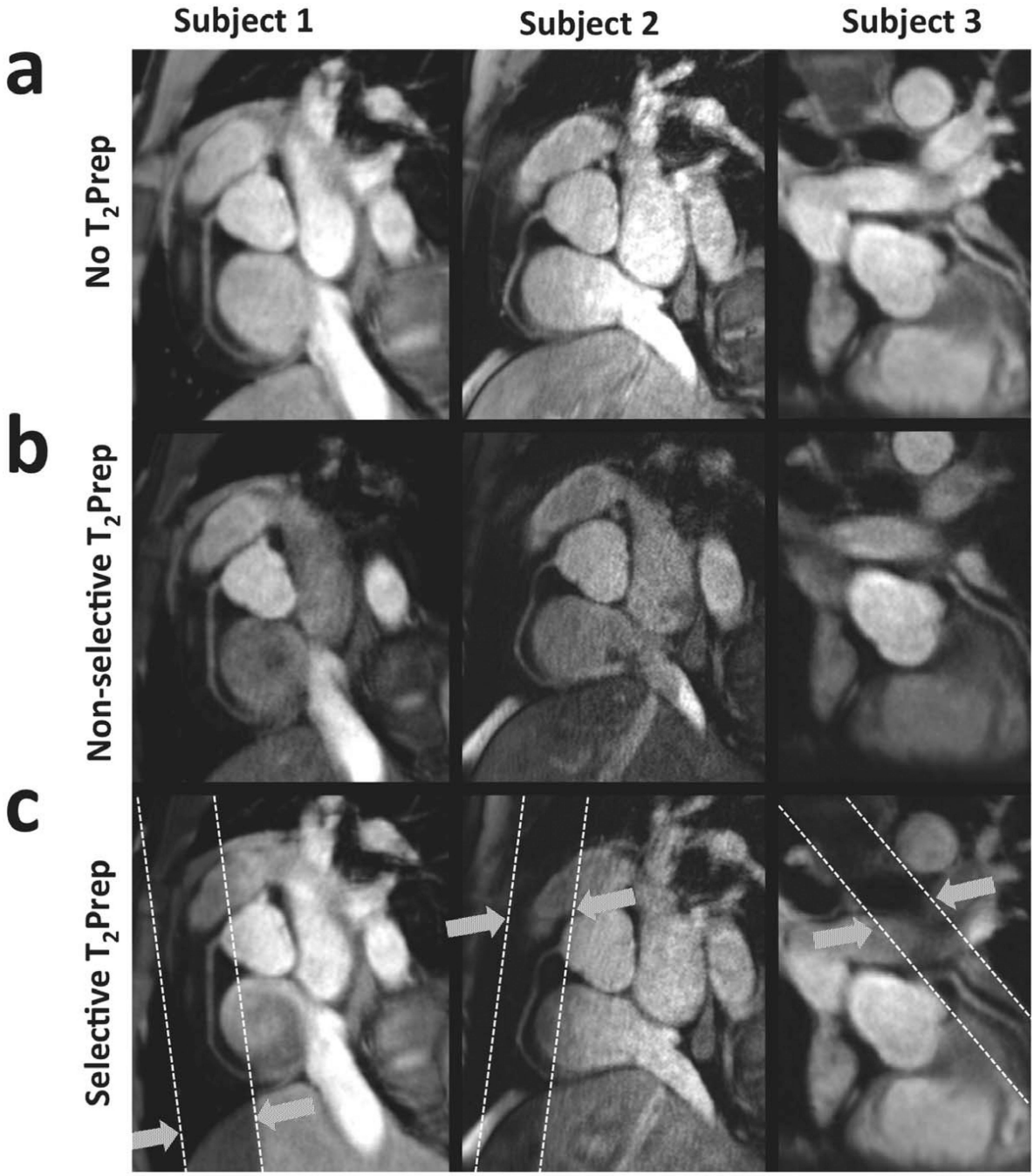

Figure 3.

Examples of RCA and LAD in three subjects using **(a)** no T_2Prep contrast, **(b)** non-selective T_2Prep, and **(c)** spatially-selective T_2Prep with T_{gap} = 150ms. Dotted white lines illustrate the orientation of the selective pre-pulse relative to the imaged volume.

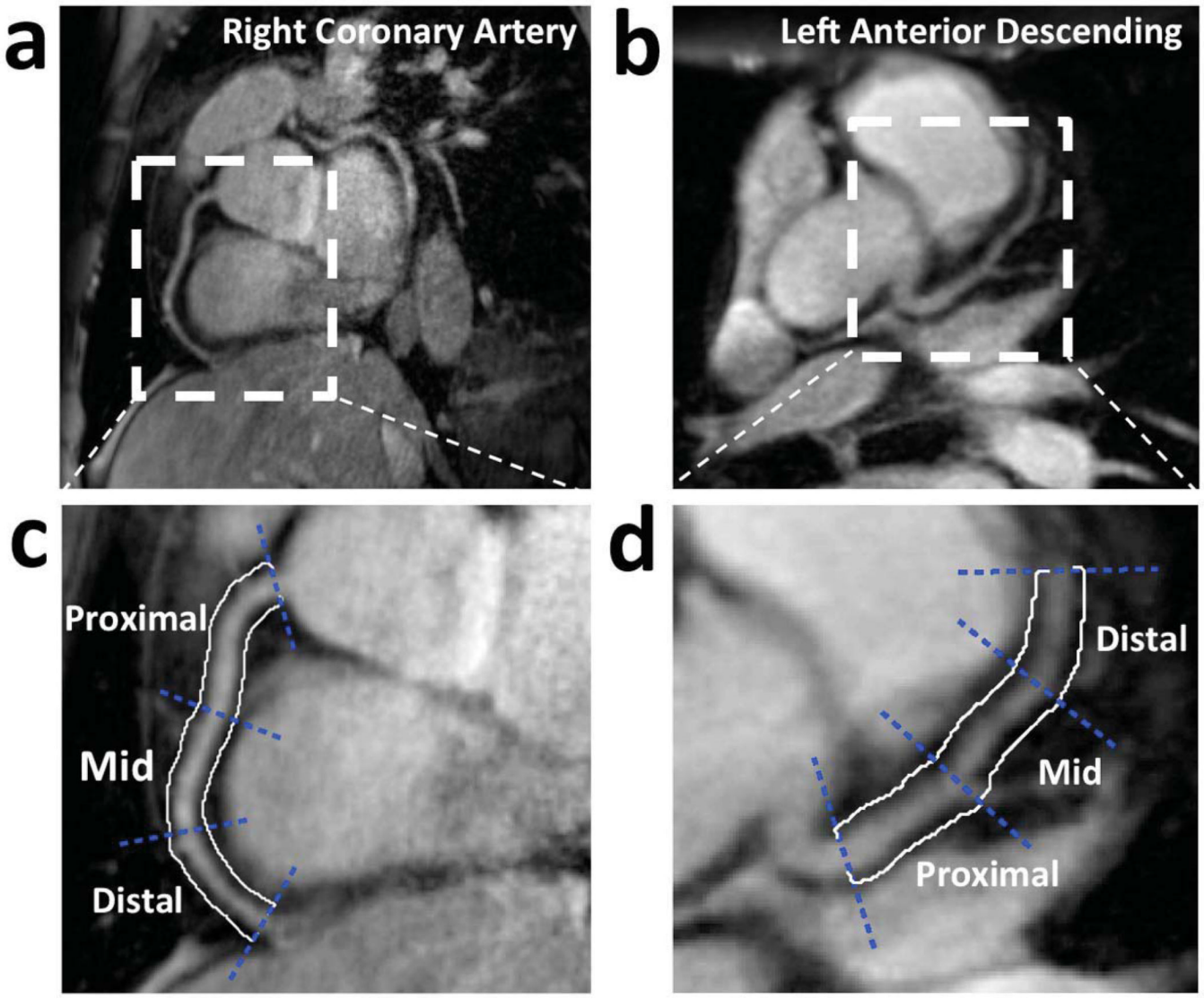

Figure 4.
Examples of **(a)** RCA and **(b)** LAD, and their proximal, mid, and distal coronary artery segments **(c)** and **(d),** respectively. White contours illustrate the vessel surroundings used for vessel-neighborhood contrast assessment.

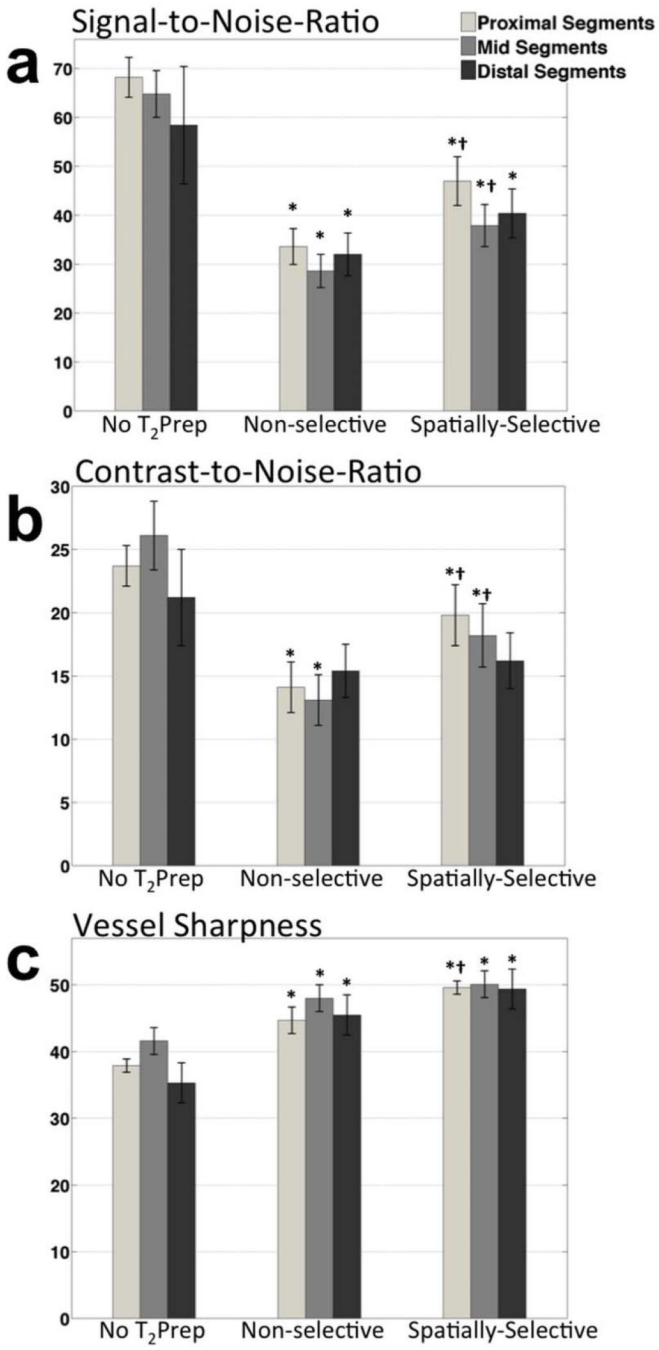

Figure 5.

(a) Vessel SNR, **(b)** vessel-neighborhood CNR, and **(c)** vessel sharpness values of the three arterial segments averaged in 22 coronary arteries. The proximal and mid coronary segments were visible in every dataset and the distal segments were identified in 8 datasets. Bar plots represent mean values and error bars represent standard error of mean (SEM). *$p<0.05$ vs. no T_2Prep; †$p<0.05$ vs. non-selective T_2Prep.

Table 1

Mean ± standard error of mean (SEM) of vessel SNR, vessel-neighborhood CNR and vessel sharpness averaged in 22 coronary arteries using no T_2Prep, non-selective T_2Prep and spatially-selective T_2Prep (T_{gap} = 150ms).

	SNR	CNR	Vessel Sharpness%
No T_2Prep	65.4±3.2	24.3±1.4	38.9±1.2
Non-selective T_2Prep	31.4±2.2 *	13.9±1.2 *	46.2±1.2 *
Spatially-selective T_2Prep	42.3±2.9 *†	18.6±1.5 *†	49.8±0.9 *

* $p<0.05$ vs. no T_2Prep.

† $p<0.05$ vs. non-selective T_2Prep.